

©2017  
Timo Roehrs  
ALL RIGHTS RESERVED

**ENCAPSULATION OF MESENCHYMAL STEM CELLS AS A POTENTIAL  
TREATMENT FOR STROKE, MODELED AS AN OXYGEN GLUCOSE  
DEPRIVED SYSTEM**

BY

**TIMO ROEHRS**

A thesis submitted to

The Graduate School-New Brunswick

And

The Graduate School of Biomedical Sciences

Rutgers, The State University of New Jersey

In partial fulfillment of the requirements

For the degree of

Masters of Science

Graduate Program in Biomedical Engineering

Written under the direction of

David I. Shreiber, And Martin L. Yarmush,

And approved by

---

---

---

---

New Brunswick, New Jersey

January 2017

## **ABSTRACT OF THE THESIS**

Encapsulation of mesenchymal stem cells as a potential  
treatment for stroke, modeled as an oxygen glucose  
deprived system  
by **Timo Roehrs**

Thesis Director:

David I. Shreiber, Ph.D. and Martin L. Yarmush Ph.D.

During a stroke there is a reduction of oxygen, glucose, and other nutrients to the surrounding brain tissue causing neuronal death and astrocyte activation. Astrocytes are responsible for protecting the neurons during an injury. Part of the astrocyte activation is the release of various molecules as well as a change in morphology from a polygonal to a stellate state. Astrocyte's morphological change can eventually lead to a glial scar preventing neurons from reforming connections. Obtaining an effective therapeutic to reduce the negative effects of astrocyte activation could greatly enhance recovery after a stroke. Mesenchymal stem cells (MSCs) have numerous anti-inflammatory and neuroprotective properties and with further development may be developed into an effective therapeutic. MSCs have been shown to regulate the immune response by reducing inflammatory molecules, such as TNF- $\alpha$ . However, there are several limitations with MSCs that must be addressed first, such as low viability, differentiation, and migration away from the injury site.

To overcome these limitations the MSCs are encapsulated in alginate. The encapsulation still allows for soluble factors to interact with the MSCs and the host tissue while maintaining

viability, keeping the MSCs undifferentiated, and allowing for localization to the injury site. In previous experiments, using encapsulated MSCs, attenuation of neuro-inflammation was achieved by PGE<sub>2</sub> secreted by the MSCs. With the encapsulated MSCs, the MSCs can be used as a therapeutic. Stroke is one injury that has few treatments where MSCs could be beneficial. *In vitro* stroke is modeled as an oxygen glucose deprived system. Rat cerebral astrocytes are plated into a 24 well plate and exposed to 1% O<sub>2</sub> and no glucose for 2.5, 5, or 10 hours. Astrocytes are then placed into normoxia conditions and recover for 24 hours.

Increased expression of GFAP and elongation of astrocytes, measured by perimeter over area signify a change to a reactive state. There is a significant difference ( $p < 0.05$ ) in a perimeter to area ratio when astrocytes are exposed to OGD compared to control. Both monolayer and encapsulated MSC reduced the perimeter to area ratio of astrocytes exposed to OGD to a control level. GFAP intensity increased after OGD exposure, but MSCs treatment did not significantly reduce GFAP intensity.

Given that PGE<sub>2</sub> was previously demonstrated to reduce LPS mediated neuro-inflammation, it was hypothesized that PGE<sub>2</sub> produced by the MSCs would also reduce GFAP intensity reduction and morphological changes. Total PGE<sub>2</sub> levels decreased with OGD, and monolayer MSCs treatment restored PGE<sub>2</sub> levels. Encapsulated MSCs increased the total PGE<sub>2</sub> levels. However, these differences are not significantly different than control. There is no difference in GFAP intensity with astrocytes exposed to exogenous PGE<sub>2</sub> during recovery.

These *in vitro* studies demonstrate that encapsulated MSCs are a viable option for reducing not only LPS mediated increase in neuro-inflammation, but also astrocyte activation. However, PGE<sub>2</sub> did not mediate astrocyte attenuation. The mechanism of reducing astrocyte activation is still not understood and further studies are needed.

## **ACKNOWLEDGEMENTS**

I want to thank Dr. David Shreiber and Dr. Rene Schloss for their guidance during this thesis. Both have given me valuable advice and support during my thesis. I would also like to thank Dr. Li Cai and Dr. Martin Yarmush for being on my committee.

I would also like to thank my parents for their support and pushing me to continue through with my education.

## TABLE OF CONTENTS

<b>ABSTRACT OF THE THESIS.....</b>	<b>ii</b>
<b>ACKNOWLEDGMENTS.....</b>	<b>iv</b>
<b>TABLE OF CONTENTS.....</b>	<b>v</b>
<b>LIST OF FIGURES.....</b>	<b>vi</b>
 <b>CHAPTER 1: INTRODUCTION.....</b>	 <b>1</b>
1.1 Role of Astrocytes During An Injury.....	1
1.2 Mesenchymal stem cells.....	2
1.3 Hypothesis.....	3
 <b>CHAPTER 2: MATERIALS AND METHODS.....</b>	 <b>5</b>
2.1 Primary Cell Culture.....	5
2.2 Human Mesenchymal stem cells.....	5
2.3 Mesenchymal stem cell alginate encapsulation.....	6
2.4 OGD Injury.....	7
2.5 MSCS, PGE <sub>2</sub> , and BDNF treatment.....	7
2.6 Cytokine analysis.....	8
2.7 Fixation and immunostaining.....	8
2.8 GFAP analysis.....	8
2.9 HIF-1 $\alpha$ .....	9
2.10 Morphology of Astrocytes.....	9
2.11 Statistical Analysis.....	10
 <b>CHAPTER 3: RESULTS.....</b>	 <b>11</b>
3.1 Base model characterized: Hif-1 $\alpha$ .....	11
3.2 GFAP expression.....	12
3.3 Morphological changes in astrocytes.....	14
3.4 Monolayer MSCS.....	16
3.5 Encapsulated MSCs.....	19
3.6 TNF- $\alpha$ .....	21
3.7 PGE <sub>2</sub> .....	21
 <b>CHAPTER 4: DISCUSSION/CONCLUSION.....</b>	 <b>25</b>
4.1 OGD.....	25
4.2 Monolayer MSCs VS Encapsulated MSCs.....	26
4.3 PGE <sub>2</sub> Response.....	27
4.5 <i>In Vivo</i> Studies.....	27
4.6 Future Studies.....	29
 <b>REFERENCES.....</b>	 <b>31</b>
 <b>APPENDIX.....</b>	 <b>33</b>
Matlab Code.....	33

## LIST OF FIGURES

<b>Figure 1.</b> Diagram representing how the images for GFAP positive astrocytes were processed. A) Represents the original image, B) represents the mask, C) represents the multiplied image of A and B, and D) represents the intensity value of GFAP positive staining as a percent number.....	9
<b>Figure 2.</b> HIF-1 $\alpha$ immunostaining of rat astrocytes and analysis. <b>A)</b> HIF-1 $\alpha$ (red) immunostaining of rat astrocytes exposed to hypoxia for 0 (control), 2.5, 5, and 10 Hrs with no recovery. Astrocytes also stained with DAPI (blue). <b>B)</b> Quantification of HIF-1 $\alpha$ immunostaining by normalized percent nuclear positive cells. Images are representative images and quantification is an N=3 with each N having 3 triplicates. Error bars are standard deviation. * P $\leq$ 0.05 compared to control.....	12
<b>Figure 3.</b> Immunoflorscent staining for GFAP (green) in astrocytes exposed to OGD with a 24 hr recovery period. Astrocytes were stained with nuclear stain DAPI (blue). These images are representative images for each condition: control, 2.5, 5, 10 hrs of OGD with 24 hr recovery.....	13
<b>Figure 4.</b> Histogram graph of control, 2.5, 5, 10 Hrs of OGD with recovery. GFAP positive pixels binned into a low and high intensity bin. OGD increases the percent of high intensity pixels compared to control for all durations. * P $\leq$ 0.05 compared to control.....	14
<b>Figure 5.</b> Astrocytes stained with GFAP (green) and DAPI (blue). <b>A)</b> Control astrocytes with a zoomed in view below. Astrocytes in a polygonal state. <b>B)</b> Astrocytes exposed to 10 hours of OGD with recovery with a zoomed in view below.....	15
<b>Figure 6.</b> <b>A)</b> Average perimeter over area ratio for control. 2.5, 5, 10 hrs of OGD with recovery. <b>B)</b> Histogram of 270 cells per condition analyzed binned at 0.05 increments. * P $\leq$ 0.05 compared to control.....	16
<b>Figure 7.</b> GFAP immunostaining (green) and DAPI (blue) for astrocytes treated with and without monolayer MSC after OGD. Representative images of astrocytes stained for GFAP. Monolayer MSC treatment has a reduction in GFAP intensity compared to no treatment.....	17
<b>Figure 8.</b> GFAP intensity analysis of control, OGD only, and OGD with monolayer MSC treatment for 2.5, 5, and 10 hours of OGD. For each duration of OGD there is a clear increase in low intensity GFAP with monolayer MSCs treatment. *P $\leq$ 0.05 compared to control. ** P $\leq$ 0.05 compared to OGD only.....	18
<b>Figure 9.</b> Morphology analysis of astrocytes by perimeter over area exposed to 0, 2.5, 5, and hours of OGD with and without monolayer MSCs treatment. Monolayer MSCs treatment reduces perimeter over area ratio to that of a control level. *P $\leq$ 0.05 compared to control. ** P $\leq$ 0.05 compared to OGD only.....	19
<b>Figure 10.</b> GFAP immunostaining (green) and DAPI (blue) for astrocytes treated with and without encapsulated MSC after OGD. Representative images of astrocytes stained for GFAP. Encapsulated MSCs treatment has a reduction in GFAP intensity compared to control.....	20

<b>Figure 11.</b> GFAP intensity analysis of control, OGD only, and OGD with encapsulated MSC treatment for 2.5, 5, and 10 hours of OGD. * $P \leq 0.05$ compared to control. ** $P \leq 0.05$ compared to OGD only.....	20
<b>Figure 12.</b> Morphology analysis of astrocytes by perimeter over area exposed to 0, 2.5, 5, and hours of OGD with and without encapsulated MSCs treatment. Monolayer MSCs treatment reduces perimeter over area ration to that of a control level. * $P \leq 0.05$ compared to control. ** $P \leq 0.05$ compared to OGD only.....	21
<b>Figure 13.</b> Total $PGE_2$ levels for 2.5, 5, and 10 hours of OGD for control, monolayer MSCs, and encapsulated MSCs. $PGE_2$ levels are normalized to control.....	22
<b>Figure 14.</b> GFAP immunostaining (green) and DAPI (blue) for astrocytes treated with and without exogenous $PGE_2$ . Representative images for each condition are shown. Images for 2ng/ml of $PGE_2$ were chosen since this was near the total $PGE_2$ level seen in the supernatant.....	23
<b>Figure 15.</b> GFAP intensity analysis of astrocytes after being exposed to exogenous $PGE_2$ during the recovery period. Concentrations of 0, 1, 2, 8, and 16 ng/ml of $PGE_2$ was used.....	24



## **CHAPTER 1: INTRODUCTION**

Stroke is a major concern for the elderly, and as the general population becomes more obese, there is an increased chance of a stroke. Symptoms of a stroke are slurred speech, facial droop, and loss of motor control<sup>1</sup>. A stroke occurs when plaque breaks off of the blood vessels and forms a clot in a blood vessel in the brain. The clot creates an environment where there is little to no oxygen and no nutrients present in the surrounding tissues. Additionally, there is little blood flow, causing for cellular waste to build up. These all can then lead to neuronal cell death. Along with neuronal death, there is activation of astrocytes, which are supporting cells to the neurons. Astrocytes can become activated during injuries and form a glial scar, which prevents the reformation of neuronal connections and hinders recovery<sup>2</sup>. Therefore, there is a need to prevent the formation of the glial scar while maintaining the positive effects of the astrocytes during injury.

### **1.1 ROLE OF ASTROCYTES DURING AN INJURY**

The role of the astrocytes before, during, and after injury has become an area of interest and target for treatments. When a neuron becomes injured, neurons release glutamate along with other neurotransmitters. This creates an environment of excitotoxicity, to the other surrounding neurons that might have previously been injured. However, due to this excitotoxicity, a cascade is created where other neurons now become injured and release even more molecules. Astrocytes help maintain the neurons by absorbing excessive neurotransmitters and calcium to allow for the neurons to continue to function normally<sup>3</sup>. By absorbing the neurotransmitter, astrocytes limit the area of the brain that is affected by the injury. However, the astrocytes also undergo changes and release various molecules. The astrocytes change morphology from a polygonal shape to a stellate shape. This change in the astrocytes is called astrogliosis<sup>4</sup>. This change in morphology can eventually lead to a glial scar, which creates a barrier that can section

off an area of the brain preventing neurons from forming connections<sup>3</sup>. Furthermore, astrocytes release various molecules, such as tumor necrosis factor alpha (TNF- $\alpha$ ), brain derived neurotrophic factor (BDNF), and molecules from the interleukin family, such as IL-6. Continued secretion of these molecules can lead to further neuronal death. Therefore, there is a need to reduce the duration of secretions of molecules, like TNF- $\alpha$ , which can help reduce the amount of neuronal death<sup>5</sup>.

Another important molecule in astrocytes is glial fibrillary acidic protein (GFAP). GFAP is an intermediate filament, specific for astrocytes, that provide structure to the astrocytes. However, GFAP also plays a role in reactivity. There is an increase in GFAP expression during astrogliosis allowing for GFAP to be used as common marker to define an astrocyte state<sup>1</sup>.

## **1.2 MESENCHYMAL STEM CELLS**

Currently, the only treatment for a stroke is to break up the clot with tissue plasminogen activator (tPA). TPA needs to be administered to the patient within the first 3-4.5 hours otherwise it cannot be administered<sup>6</sup>. However, there is no effective treatment for the secondary effects from the blood clot, but one possible treatment could be the use of mesenchymal stem cells (MSCs). MSCs has several disadvantages when used by themselves, such as differentiation, viability, and mobility away from the injury site. One solution to these disadvantages is to encapsulate the MSCs in alginate. This has been extensively studied in the Yarmush lab group. Briefly, the viability of the MSCs was assessed over time up to 60 days post encapsulation, resulting in >90% viability in alginate<sup>8</sup>. Additionally, a panel of cytokines and growth factors was evaluated between monolayer and encapsulated MSCs. At a 2.2% alginate concentration, there is a small increase in cytokine production compared to monolayer MSCs. For example, after 2 days of encapsulation, there is an increase in IL-2, IL-10, and VEGF<sup>6</sup>. Additionally, MSCs was shown to modulate T-cell immunological responses through the production of PGE<sub>2</sub> and when stimulated

by LPS or TNF- $\alpha$  could modulate macrophages through PGE<sub>2</sub><sup>9, 10</sup>. Furthermore, 1.7%, 2.2%, and 2.5% alginate capsules were tested. Using 2.2% alginate was able to maintain the current state of the MSCs better than 2.5%. 1.7% were also able to maintain the MSCs, but was not chosen for further evaluation because 2.2% was previously used in other experiments<sup>8</sup>.

Mesenchymal stem cells have previously been shown to modulate inflammation in the nervous system<sup>7</sup>. Additional benefits of the alginate capsules are that they are inert to astrocytes, keep the MSC localized, and provide a barrier keeping MSCs out of direct contact with the astrocytes while still allowing for exchanges in oxygen, carbon dioxide and other wastes, and various proteins such as PGE<sub>2</sub>. Additionally, MSCs have been extensively studied in regulating macrophages. The base secretome of the MSC have been analyzed, including their response to lipopolysaccharide (LPS) activated astrocytes<sup>11</sup>. In this study, astrocytes were activated with LPS and then had a monolayer or alginate encapsulated MSCs co-culture in order to reduce the amount of tumor necrosis factor alpha (TNF- $\alpha$ ) produced by astrocytes<sup>11</sup>. TNF-  $\alpha$  is an inflammatory protein that is often produced in response to LPS. This signified that the MSCs was producing something in response to the TNF-  $\alpha$ . Upon further investigation, this factor was PGE<sub>2</sub>. In this model and previous models, the alginate encapsulated MSCs performed better than monolayer MSCs in regulating inflammatory molecules.

Current research on MSCs have shown that they improve viability in astrocytes via the Bcl-2 pathway during OGD<sup>12</sup>. However, which paracrine factors the MSCs are producing to cause this change has not been determined. There has been little focus on HIF-1 $\alpha$  expression during OGD, GFAP expression, or the changes in morphology to the astrocytes. HIF-1 $\alpha$  has the potential to quantify the extent of hypoxia.

### **1.3 HYPOTHESIS**

One downfall with LPS, is that it is an artificial means of creating an inflammatory response in astrocytes. Therefore, there is a need to examine the effectiveness of the MSCs in a more relevant injury environment. This led to the examination of the effectiveness of the MSCs on astrocytes in an OGD environment which models stroke *in vitro*. By determining that the MSCs retain their effectiveness in an OGD model will allow for the use of MSCs to continue to even more relevant models such as tri-culture with neurons, organotypic slice cultures, or an *in vivo* stroke models. The hypothesis is that the MSCs will modulate the reactivity of the astrocytes and that alginate encapsulated MSCs will perform equal to or better than a monolayer MSCs.

## **CHAPTER 2: MATERIALS AND METHODS**

### **2.1 PRIMARY CELL CULTURE**

All animal procedures were approved by Rutgers animal committee (Piscataway, NJ). Astrocytes are obtained from Sprague-Dawley rat pups (Taconic Biosciences Inc.) postnatal 2-3 days as previously described<sup>13</sup>. In short, the rat pups were decapitated and the skin on top of the skull was removed by using scissors. The brain was then lifted out with forceps and placed in a petri dish with ice cold dissection media, Hanks' balanced salt solution (Sigma-Aldrich). The two hemispheres are then separated and the cerebral cortices isolated. The meninges are removed. The tissue is then diced into small pieces and incubated with 0.1% trypsin (Sigma-Aldrich) and 0.02% DNase (Sigma-Aldrich) for 20 minutes. The tissue is then triturated several times until a cell suspension is obtained. The cell suspension is washed twice with DMEM (Sigma-Aldrich) +10%FBS (Atlanta Biologicals) and filtered through a 40um nylon mesh. The cell suspension is then centrifuged at 1000 RPM for 5 minutes and then placed into a 75cm<sup>2</sup> culture flask with 10ml culture media (DMEM + 1% pen/strep (Sigma-Aldrich) + 1% L glutamine (Sigma-Aldrich) + 10%FBS). After 6-7 days the astrocytes become confluent and are trypsinized with 0.25% trypsin EDTA (Sigma-Aldrich) and used for experiments or passaged. Passages 1 and 2 were used for experiments.

### **2.2 HUMAN MESENCHYMAL STEM CELLS**

Human bone-marrow mesenchymal stromal cells from donor 2 purchased from Texas A&M and was previously characterized<sup>8</sup>. MSCs were thawed from passage 2. The frozen MSCs is first thawed in a 37°C water bath until a small amount of ice remained. Then the MSCs was removed and had 5ml of cold MEM-alpha (Gibco) with 10% FBS, 1% penicillin streptomycin, 1% L-glutamine, and 1ng/ml human fibroblast growth factor (Gibco) added dropwise. 1ml of the solution was added back to the cryovial to get all cells out. The MSCs was then centrifuged at 400

RCF for 5 minutes. MSCs was then plated into a 175cm<sup>2</sup> flask with 20ml of culture media. After 3-4 days the MSC would reach 70% confluency and was passage into two 225cm<sup>2</sup> flasks. MSCs was used between passages 3-6. Monolayer MSCs were plated 1 day prior to use in a transwells at a density of  $1.25 \times 10^4$  cells. The final density of the monolayer MSCs was assumed to be  $2.5 \times 10^4$  at the time of use.

### **2.3 MESENCHYMAL STEM CELL ALGINATE ENCAPSULATION**

Mesenchymal stem cells were encapsulated in alginate poly-L-lysine (PLL) as previous described<sup>7</sup>. A 2.2% (w/v) alginate solution was made with no glutamine, no calcium, high glucose DMEM. Previously cultured MSCs were disassociated from the culture flask and re-suspended in the 2.2% alginate solution with 90% alginate solution and 10% no calcium, no glutamine, high glucose DMEM at a seeding density of  $2 \times 10^6$  cells/ml. This concentration and seeding density has been previously determined to maintain cell viability and maintain the MSC in an undifferentiated state<sup>6</sup>. The alginate solution was then extruded through a 500uM needle into a crosslinking solution to create capsules of approximately 400uM. The crosslinking solution is made up of D-+-Glucose (Sigma-Aldrich) 13.8mM, NaCl (Sigma-Aldrich) 145mM, MOPS (Sigma-Aldrich) 10mM, CaCl<sub>2</sub> (Sigma-Aldrich) 100mM, and DI water. The extruder was set at a flow rate of 10ml per hour, and the electrode to 6.4kV. The capsules stay in the crosslinking solution for 10 minutes. The capsules are then washed with PBS (Gibco), filtered and washed with PLL (Sigma-Aldrich) for 2 minutes. After the PLL wash, the capsules are washed with PBS, filtered and washed with culture media. The capsules are filtered again and suspended in 5ml culture media in an upright 25cm<sup>2</sup> culture flask. MSCs capsules were then stained with propidium iodide (Molecular Probes) and DAPI (Molecular Probes) to count number of live and dead cells. Propidium iodide is a molecule that can only get into cells when the cell membrane is broken down, therefore making it a marker for dead cells. DAPI is a molecule that binds to DNA, allowing for cells to be identified.

Any cell with DAPI and no propidium iodide stain is a live cell and any cell with both DAPI and propidium iodide stain is a dead cell. Capsules were used 1 day after encapsulation. Encapsulated MSCs are plated into a transwell at  $2.5 \times 10^4$  MSCs per well.

## **2.4 OGD INJURY**

Astrocytes are used at passage 1 or 2 and are plated at  $5 \times 10^4$  cells per well in normal culture media. After 48 hours, experimental wells are washed with glucose free, serum free DMEM and control cells washed with normal culture media. After washing, experimental wells had new glucose free, serum free DMEM added that has been deoxygenated for 5 minutes and control wells had normal culture media. Deoxygenation was done by putting the culture media in a vacuum with shaking. Experimental wells were placed into a hypoxic incubator set to 1% O<sub>2</sub>, 5% CO<sub>2</sub> and 94% N<sub>2</sub>. Experimental wells were left in a hypoxic chamber for 2.5, 5, 10 hours. Control conditions were cultured in normoxia. After OGD duration, all media were collected and store for further analysis. Some wells were fixed after OGD to be tested for HIF-1 $\alpha$ . Experimental conditions had serum free DMEM media added and control conditions had normal media. All conditions were placed into normoxia for a 24 hour recovery period. After 24 hours, all media were collected and the cells were fixed for further staining.

## **2.5 MSCS, PGE<sub>2</sub>, AND BDNF TREATMENT**

All treatments were added immediately after OGD for the full duration of recovery. MSCs was added as a monolayer or encapsulated as previously described. Exogenous PGE<sub>2</sub> (Cayman Chemical) and BDNF (Peprotech) was added during the recovery period. PGE<sub>2</sub> was dissolved in sterile PBS and then diluted in serum free DMEM media to the appropriate concentration. Concentrations of 1000, 2000, 4000, and 16000 pg/ml was used. BDNF was dissolved in sterile PBS and diluted in serum free DMEM media to the appropriate concentration. Concentrations of 12.5, 25, 50, and 100 pg/ml were used.

## 2.6 CYTOKINE ANALYSIS

Media collected after OGD and after recovery was stored at -20°C. Samples were tested for rat TNF- $\alpha$  (Biolegends) and total PGE<sub>2</sub> (Cayman Chemicals) according to the manufacturer's instructions.

## 2.7 FIXATION AND IMMUNOSTAINING

All cells were fixed with 4% w/v paraformaldehyde (PFA) (Sigma-Aldrich) for 30 minutes. After 30 minutes, cells were washed with immunobuffer (1x PBS + triton-x + BSA) (Sigma-Aldrich) 3 times for 5 minutes each time. After immunobuffer, the cells were blocked with 10% normal goat serum (Sigma-Aldrich) made in immunobuffer for 1 hour. After blocking, primary antibody for GFAP was added at 1:500 for 1 hour. GFAP made in rabbit (DAKO) and GFAP made in chicken (Aves) was used. After the primary antibody, the cells were washed 3 times for 5 minutes with immunobuffer. Next a secondary goat anti-rabbit 488 (Invitrogen) or goat anti-chicken 568 (Invitrogen) was added at 1:500 for 1 hour. The cells were then washed 3 times for 5 minutes with immunobuffer. DAPI was added for 10 minutes at 2:500 and then washed 3 times for 5 minutes with immunobuffer. All antibody dilutions were done in immunobuffer. HIF-1 $\alpha$  was done in a similar manner with the following changes. The cells were blocked for 2 hours and the primary antibody is a monoclonal anti-HIF-1 $\alpha$  produced in mouse clone ESEE122 (Sigma-Aldrich) at a 1:1000 dilution. The secondary antibody was goat anti-mouse 568 (Invitrogen) at 1:1000 dilution for 2 hours.

## 2.8 GFAP ANALYSIS

Cells stained for GFAP were imaged under an inverted microscope at 10x. The intensity of the GFAP stain was compared between conditions. This was done by first thresholding the images to create a mask. The mask is then multiplied with the original image, retaining GFAP positive



stained pixel values and background values to 0. The intensity and number of pixels of positive staining was recorded (Figure 1).

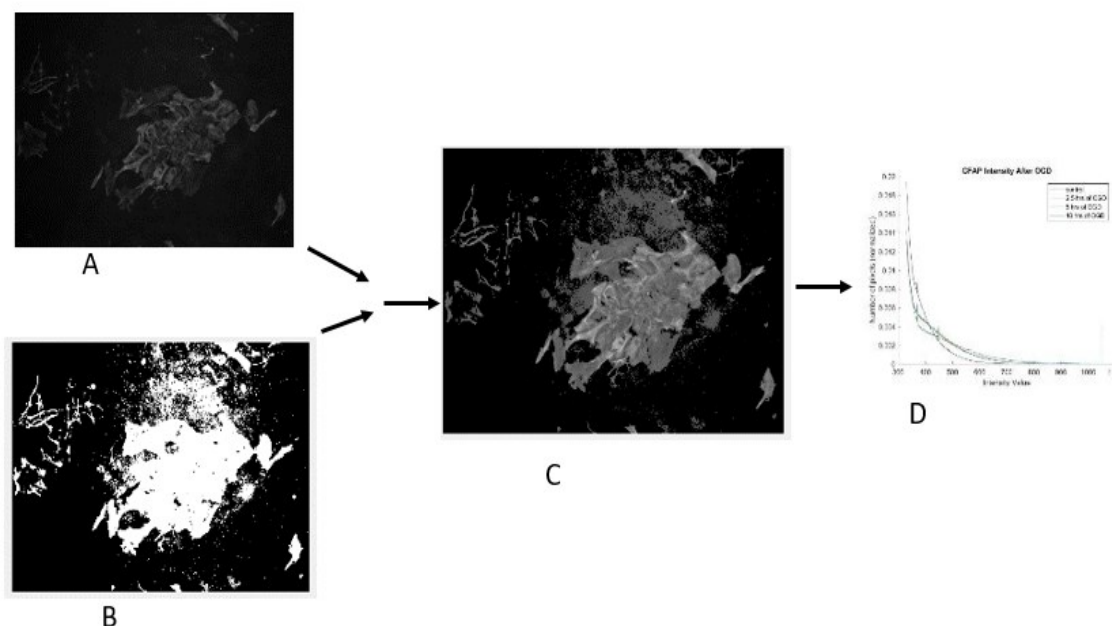


**Figure 1.** Diagram representing how the images for GFAP positive astrocytes were processed. A) Represents the original image, B) represents the mask, C) represents the multiplied image of A and B, and D) represents the intensity value of GFAP positive staining as a percent number.

9 images were captured for each condition and each experiment was repeated 3 times.

The intensity value for each GFAP positive pixel was binned into a low or high intensity bin. The low intensity pixel bin is set by having 80% of the GFAP positive pixels from the control condition falling into the low bin and the high bin having 20% of the GFAP positive pixels of control. This was done for each image and then the images were averaged together for each condition.

## 2.9 HIF-1 $\alpha$ ANALYSIS

Cells stained for HIF-1 $\alpha$  were imaged under an inverted microscope at 10x. The number of DAPI positive and nuclear HIF-1 $\alpha$  positive cells were quantified. A percent positive number was generated. This was done for 9 images for each condition repeated 3 times.

## 2.10 MORPHOLOGY OF ASTROCYTES

Using the GFAP images of the astrocytes, the perimeter and area of 10 cells per images was obtained in order to create a morphology number. The morphology number is calculated by dividing the perimeter by the area as previously done<sup>14</sup>.

### **2.11 Statistical Analysis**

All statistical analysis was performed using MATLAB. An ANOVA was performed with a post-hoc Turkey-HSD test. Groups are considered significantly different with a P value  $\leq 0.05$ . All results are a mean  $\pm$  standard deviation unless otherwise noted. OGD only, monolayer MSC, and encapsulated MSCs experiment was performed 3 times in triplicate. Exogenous PGE<sub>2</sub> experiment was performed in duplicate with triplicates.

## CHAPTER 3: RESULTS

### 3.1 BASE MODEL CHARACTERIZED: HIF-1 $\alpha$

The literature has different ways of setting up an OGD system, so determining the base response of the astrocytes in this OGD system was essential<sup>15, 16</sup>. To determine if a hypoxic environment was created, the astrocytes were stained for HIF-1 $\alpha$ . Immediately after OGD exposure astrocytes were fixed and stained for HIF-1 $\alpha$ . Under normoxia, HIF-1 $\alpha$  is rapidly degraded. However, under hypoxia, HIF-1 $\alpha$  is translocated into the nucleus of the cell.

Interestingly, there was a small degree of nuclear staining in control astrocytes but a much larger degree in hypoxic exposed astrocytes (Figure 2a). Additionally, there was a decrease in the percent positive nuclear stained astrocytes with increasing hypoxic exposure (Figure 2b). 2.5 hours of OGD had 7.35 fold increase compared to control. 5 and 10 hours of OGD had a 5.29 and 3.35 fold change compared to control.

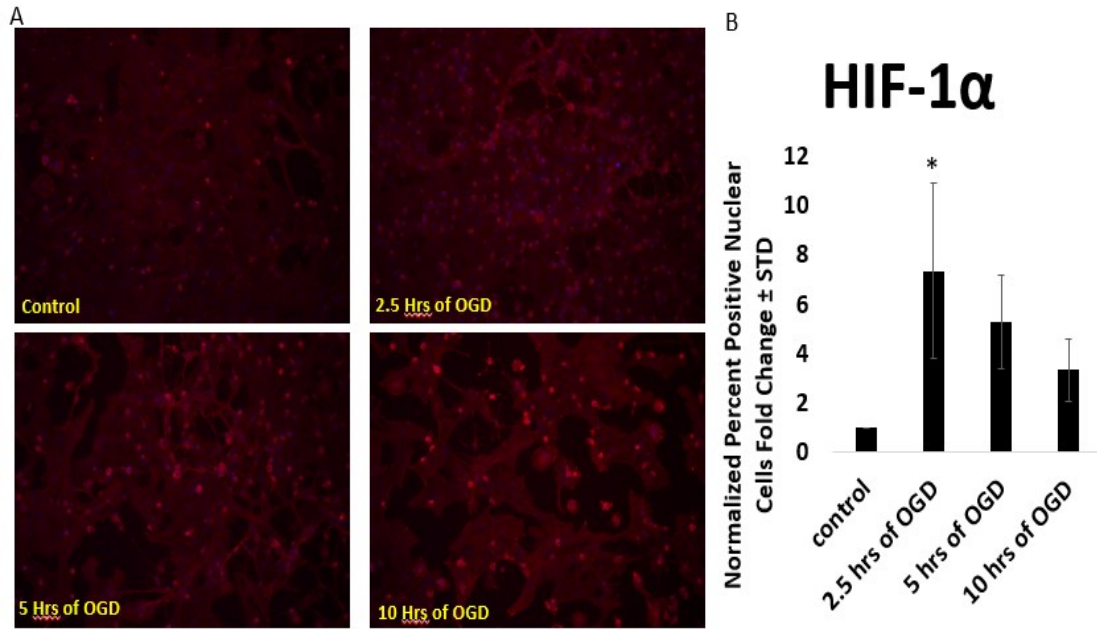


**Figure 2.** HIF-1 $\alpha$  immunostaining of rat astrocytes and analysis. **A)** HIF-1 $\alpha$  (red) immunostaining of rat astrocytes exposed to hypoxia for 0 (control), 2.5, 5, and 10 Hrs with no recovery. Astrocytes also stained with DAPI (blue). **B)** Quantification of HIF-1 $\alpha$  immunostaining by normalized percent nuclear positive cells. Images are representative images and quantification is an N=3 with each N having 3 triplicates. Error bars are standard deviation. \*  $P \leq 0.05$  compared to control.

### 3.2 GFAP EXPRESSION

Having confirmed that the astrocytes were in a hypoxic environment, astrocyte GFAP expression was evaluated. Astrocytes were stained for GFAP after OGD exposure and a 24 hour recovery period. A 24 hour recovery period was chosen based on previous studies with LPS<sup>15</sup>. Astrocytes were in an OGD environment for 2.5, 5, and 10 hours and then returned to normoxia for a 24 hours recovery period. Control astrocytes were evaluated for GFAP to obtain a baseline expression level as shown in Figure 3. With OGD there is an increase in GFAP expression as shown by immunofluorescent staining.

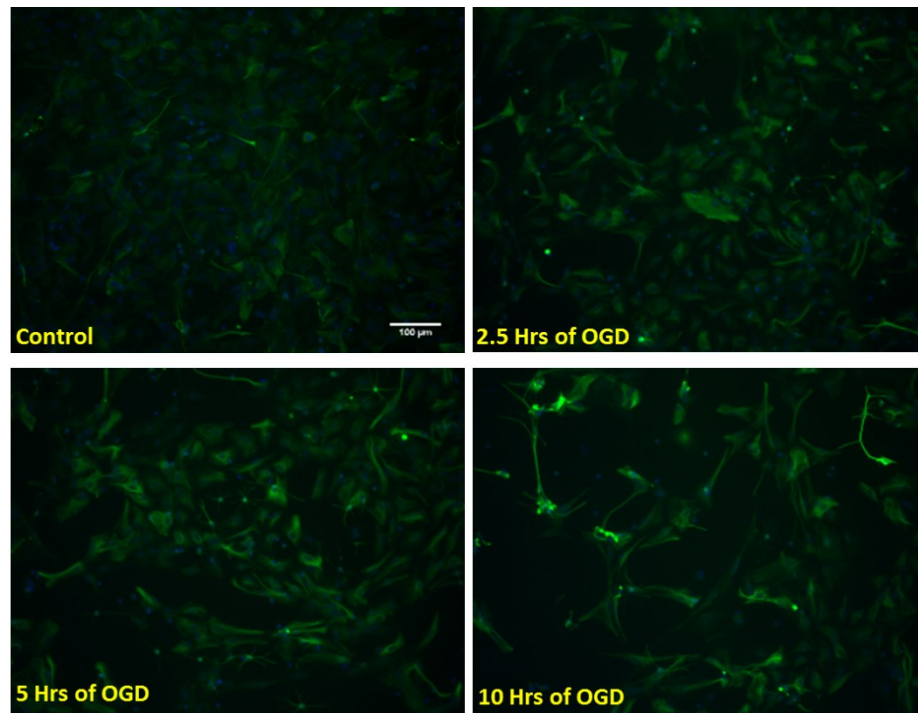


**Figure 3.** Immunofluorescent staining for GFAP (green) in astrocytes exposed to OGD with a 24 hr recovery period. Astrocytes were stained with nuclear stain DAPI (blue). These images are representative images for each condition: control, 2.5, 5, 10 hrs of OGD with 24 hr recovery.

Visually there is a difference in GFAP intensity between control and OGD exposure. To quantify this difference in GFAP staining, the GFAP positive cells were binned in a low or high intensity bin as previously stated in methods. OGD conditions have a lower percent of pixels in the low bin and a higher percent of pixels in the high bin (Figure 4). There is no time dependent response to OGD when looking at GFAP intensity. The percent number of pixels for 2.5, 5, 10 hours OGD are 0.629, 0.587, and 0.629 respectively, for the low intensity bin compared to 0.8 for control.

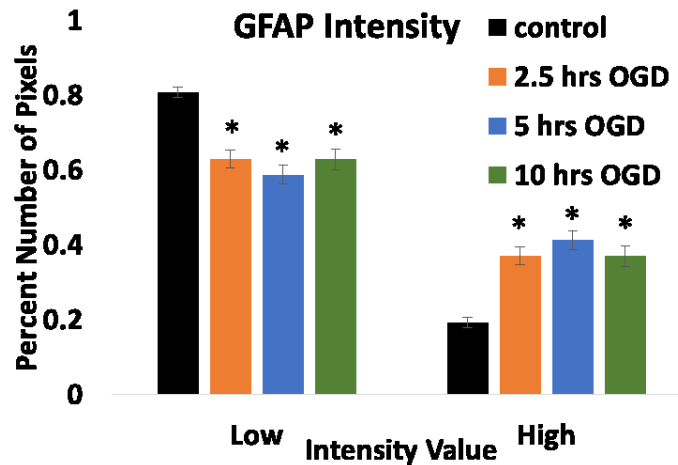


**Figure 4.** Histogram graph of control, 2.5, 5, 10 hours of OGD with recovery. GFAP positive pixels binned into a low and high intensity bin. OGD increases the percent of high intensity pixels compared to control for all durations. \*  $P \leq 0.05$  compared to control

### 3.3 MORPHOLOGICAL CHANGES IN ASTROCYTES

Next the morphology of the astrocytes was analyzed. There is a change in the astrocytes going from a polygonal state (Figure 5a) to a stellate state (Figure 5b) after OGD indicating astrogliosis. With a zoomed in view, the astrocytes exposed to OGD have become elongated.

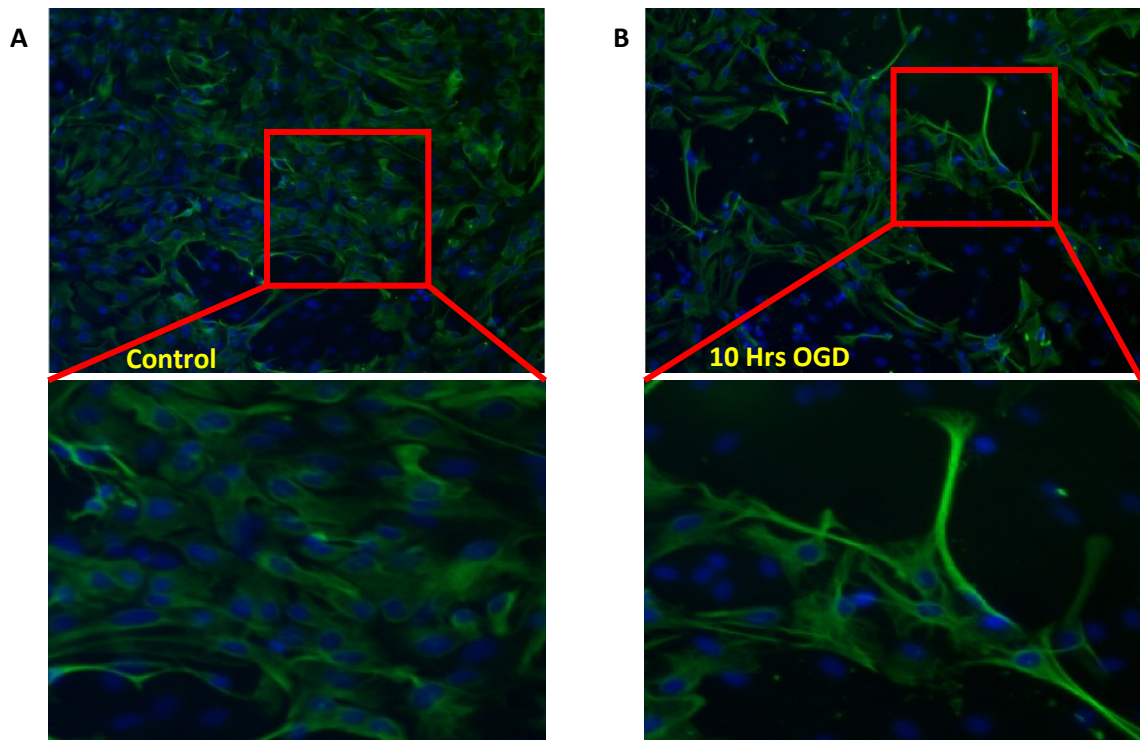


**Figure 5.** Astrocytes stained with GFAP (green) and DAPI (blue). **A)** Control astrocytes with a zoomed in view below. Astrocytes in a polygonal state. **B)** Astrocytes exposed to 10 hours of OGD with recovery with a zoomed in view below.

270 astrocytes per condition were analyzed and averaged. OGD conditions have a significant increase in morphology compared to control and a time dependent increase although not significantly. Figure 6a shows the average perimeter to area ratio and Figure 6b shows the perimeter to area ratio binned at a bin size of 0.05. The increase in average perimeter to area ratio is due to the increase in number of astrocytes having ratios larger than 0.1.

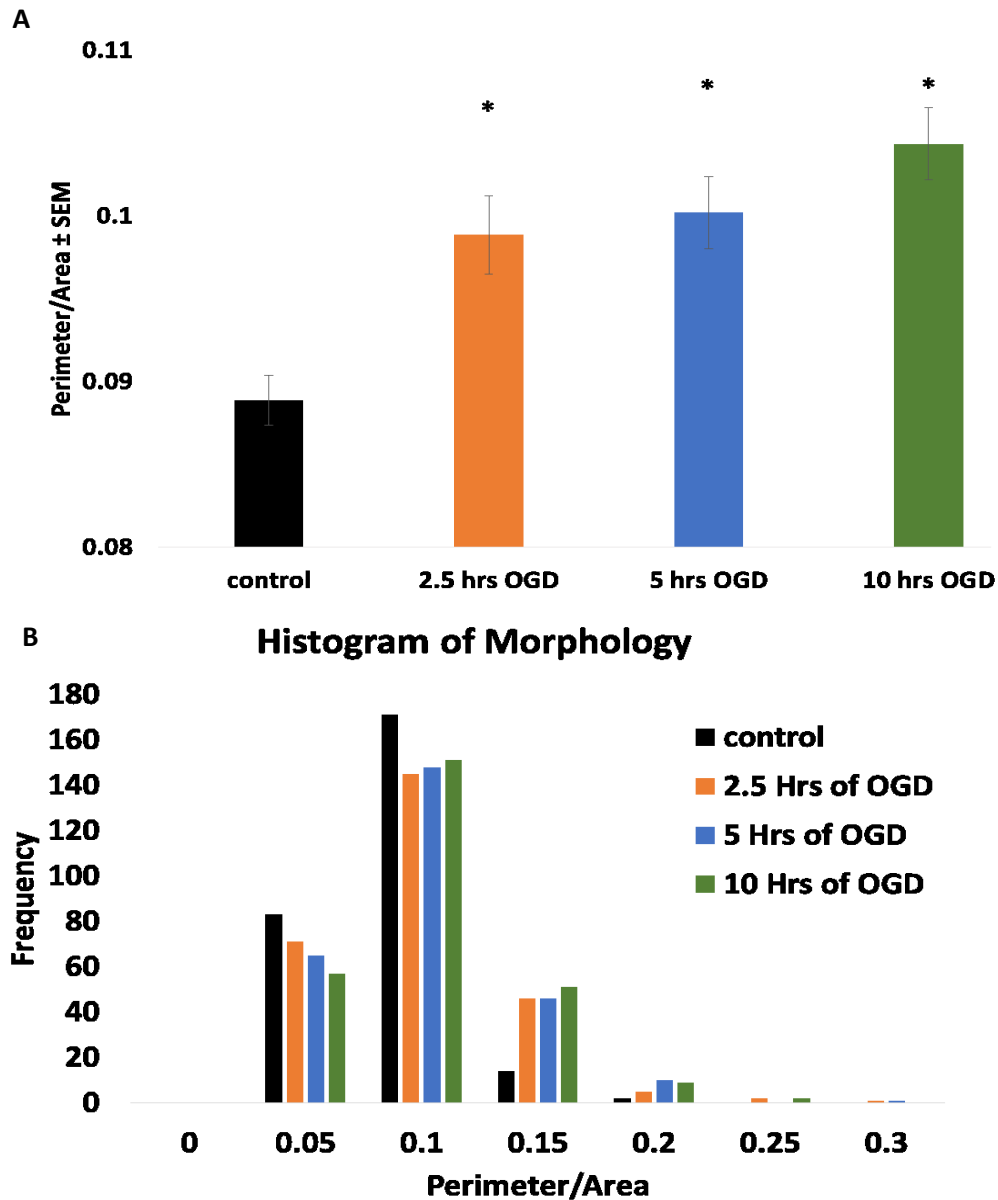


**Figure 6. A)** Average perimeter over area ratio for control. 2.5, 5, 10 hrs of OGD with recovery. **B)** Histogram of 270 cells per condition analyzed binned at 0.05 increments. \*  $P \leq 0.05$  compared to control.

### 3.4 MONOLAYER MSCS

The GFAP expression of the astrocytes was examined after a 24 hour treatment of monolayer MSCs. Figure 7 shows the images of the GFAP immunostaining with a clear decrease in GFAP staining in monolayer treated astrocytes compared to OGD only. Figure 8 shows the GFAP intensity of the various conditions grouped by OGD duration. There is a decrease in GFAP intensity



with monolayer MSCs treatment, but not to a control level intensity. 5 hours of OGD with monolayer treatment of OGD is still significantly different than control levels of OGD. 2.5 hours of OGD with monolayer treatment had 73% pixels for the low intensity bin. 5 hours of OGD with monolayer treatment had 69% pixels for the low intensity bin. 10 hours of OGD with monolayer treatment had a 70% pixels for the low intensity bin. Figure 9 shows the average perimeter to area ratio for the astrocytes as control, OGD only and OGD with monolayer treatment. Monolayer MSCs treatment reduced elongation to a control level. Control astrocytes had a ratio of 0.088 compared to 0.089, 0.095, and 0.088 for 2.5, 5, and 10 hours of OGD with monolayer treatment.

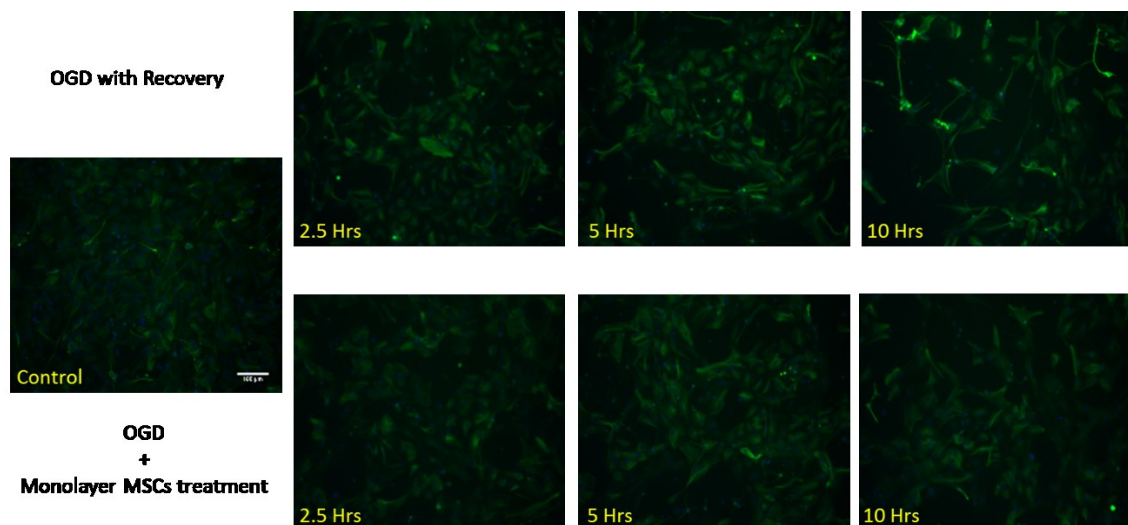


**Figure 7.** GFAP immunostaining (green) and DAPI (blue) for astrocytes treated with and without monolayer MSC after OGD. Representative images of astrocytes stained for GFAP. Monolayer MSC treatment has a reduction in GFAP intensity compared to no treatment.

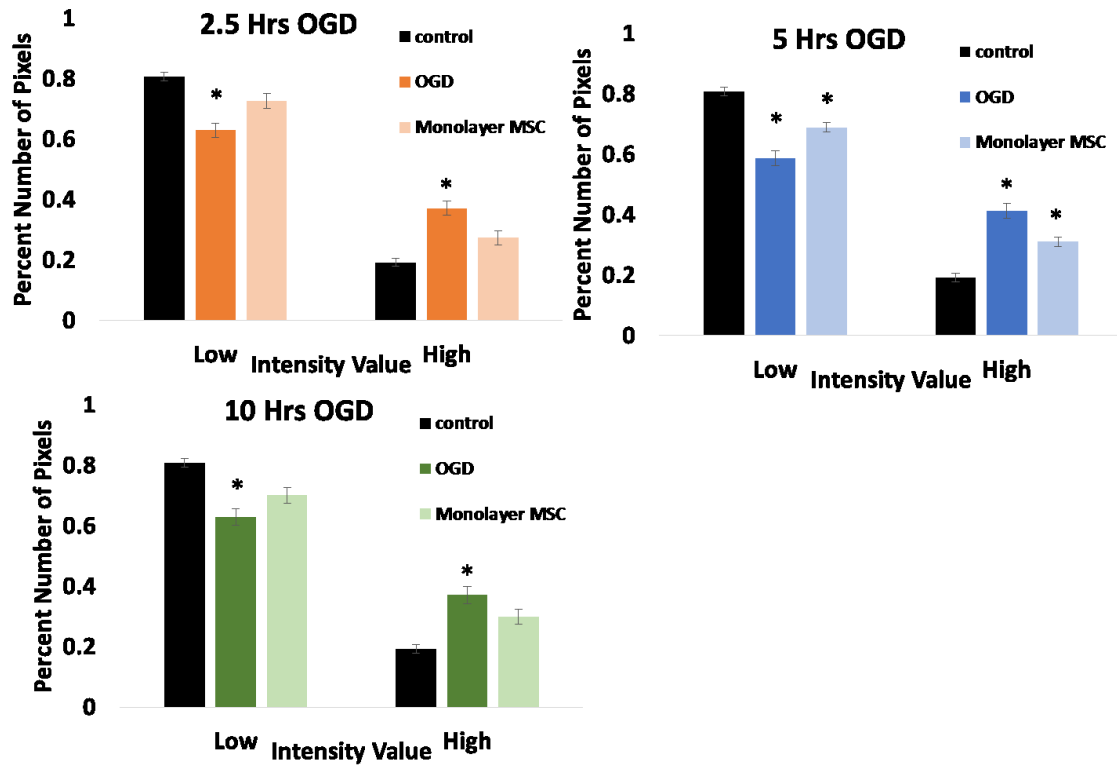


**Figure 8.** GFAP intensity analysis of control, OGD only, and OGD with monolayer MSC treatment for 2.5, 5, and 10 hours of OGD. For each duration of OGD there is a clear increase in low intensity GFAP with monolayer MSCs treatment. \* $P \leq 0.05$  compared to control. \*\*  $P \leq 0.05$  compared to OGD only.

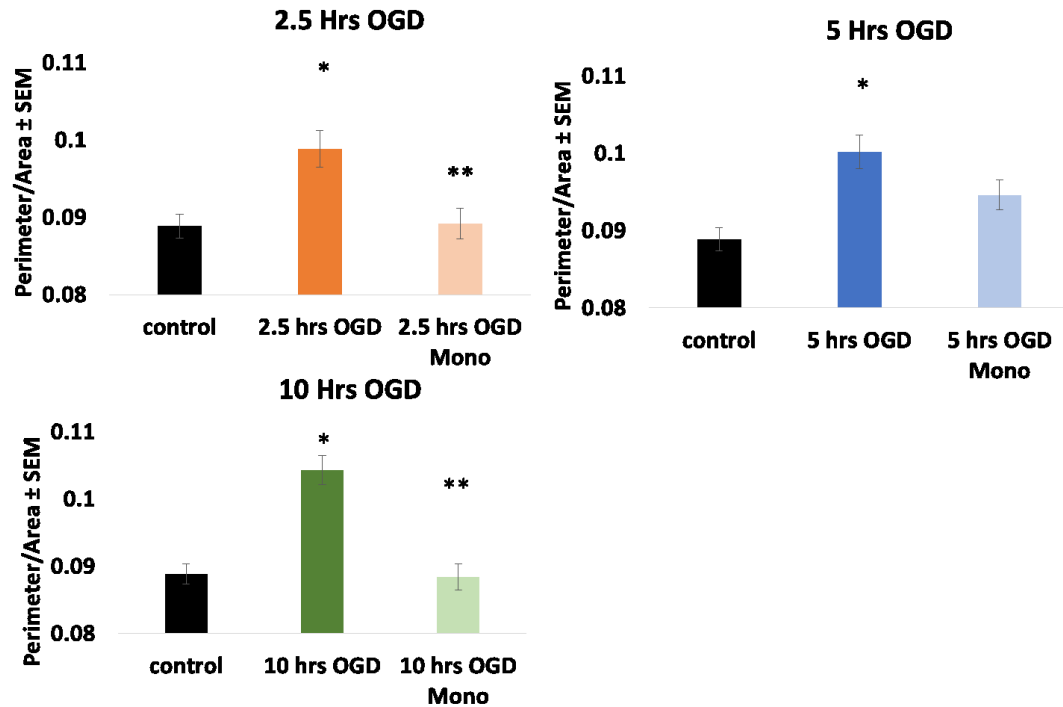


**Figure 9.** Morphology analysis of astrocytes by perimeter over area exposed to 0, 2.5, 5, and 10 hours of OGD with and without monolayer MSCs treatment. Monolayer MSCs treatment reduces the perimeter over area ratio to that of a control level. \* $P \leq 0.05$  compared to control. \*\*  $P \leq 0.05$  compared to OGD only.

### 3.5 ENCAPSULATED MSCs

Encapsulated MSCs was added after OGD during the recovery period for 24 hrs. Encapsulated MSCs reduced the GFAP intensity as seen by immunostaining (Figure 10). Control GFAP expression levels are lower than OGD only and OGD with encapsulated MSCs. Encapsulated MSCs GFAP intensity was lower than OGD only. This was consistent across all durations of OGD (Figure 11). Only 5 hours of OGD with encapsulated MSCs was significantly different than OGD only. Additionally the perimeter to area ratio was reduced with encapsulated MSC treatment for all durations of OGD (Figure 12). For each OGD duration, encapsulated MSCs reduced the perimeter to area ratio to a control level.

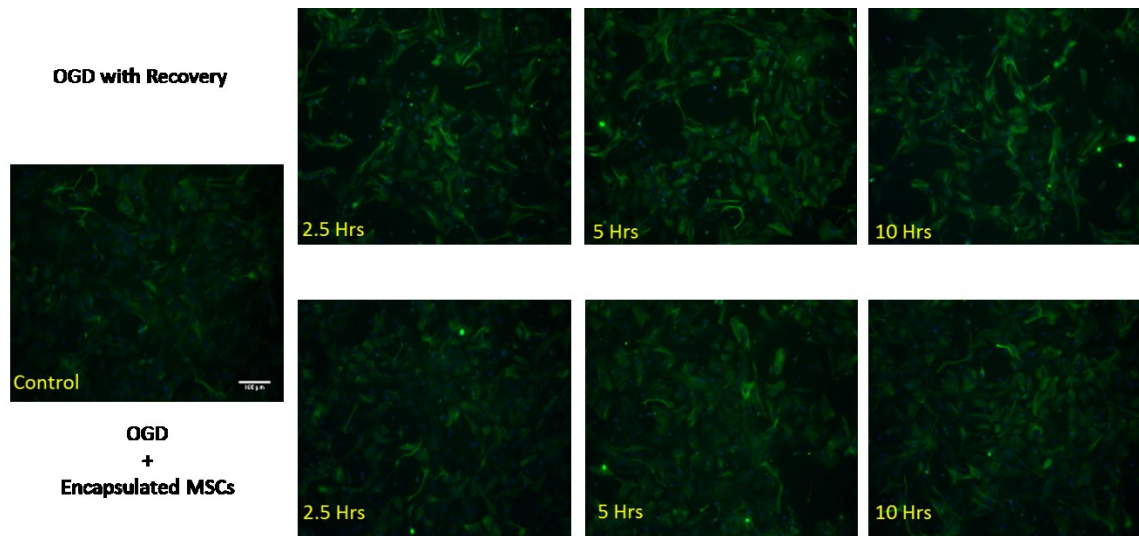


**Figure 10.** GFAP immunostaining (green) and DAPI (blue) for astrocytes treated with and without encapsulated MSC after OGD. Representative images of astrocytes stained for GFAP. Encapsulated MSCs treatment has a reduction in GFAP intensity compared to control.

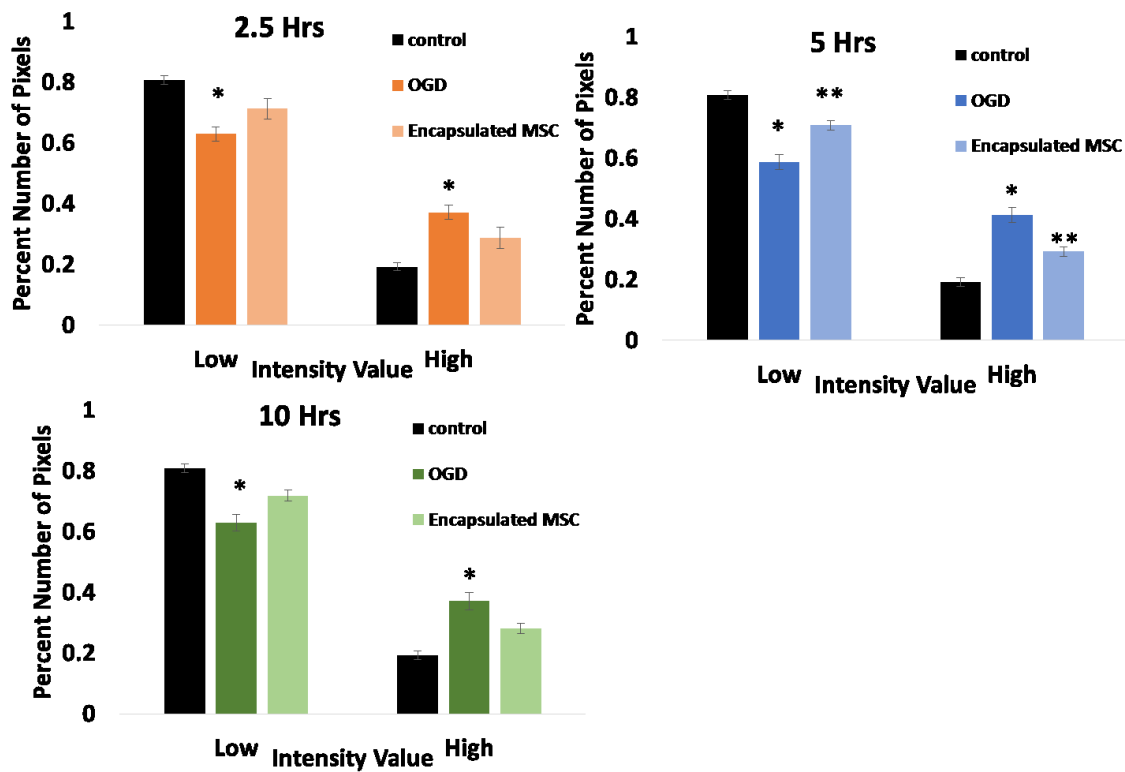


**Figure 11.** GFAP intensity analysis of control, OGD only, and OGD with encapsulated MSC treatment for 2.5, 5, and 10 hours of OGD. \* $P \leq 0.05$  compared to control. \*\*  $P \leq 0.05$  compared to OGD only.

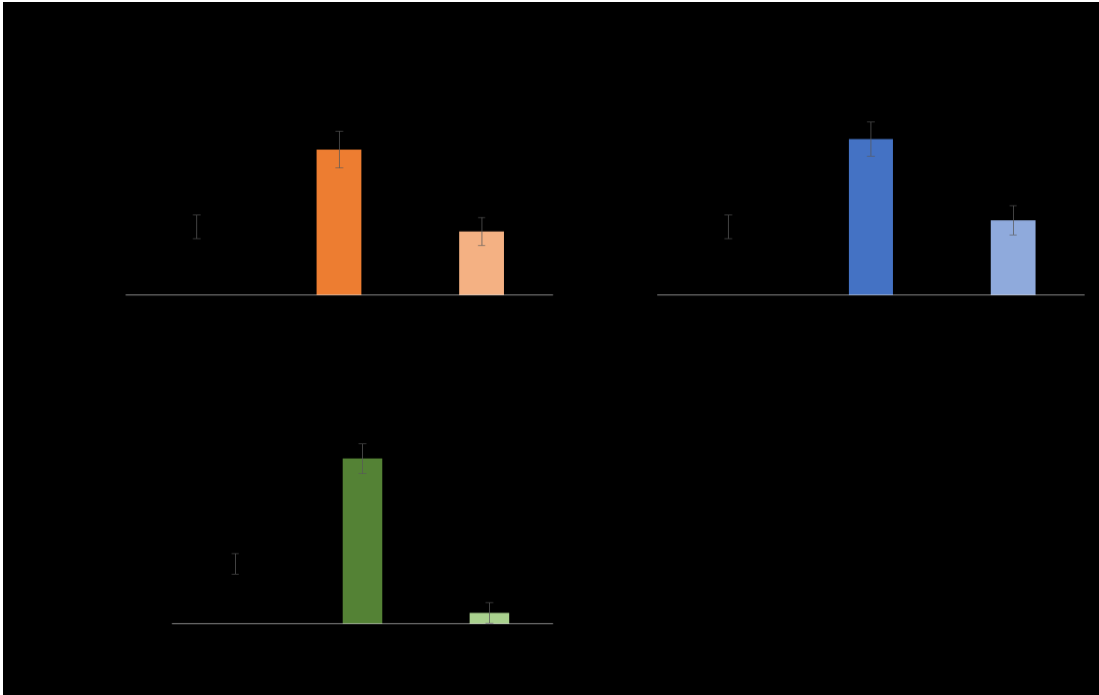


**Figure 12.** Morphology analysis of astrocytes by perimeter over area exposed to 0, 2.5, 5, and hours of OGD with and without encapsulated MSCs treatment. Monolayer MSCs treatment reduces perimeter over area ratio to that of a control level. \* $P \leq 0.05$  compared to control. \*\* $P \leq 0.05$  compared to OGD only.

### 3.6 TNF- $\alpha$

Astrocyte supernatants were tested for TNF- $\alpha$ . Supernatants collected immediately after OGD and after OGD with recovery were tested. The levels of TNF- $\alpha$  were below the standard curve and near zero for all controls, OGD conditions, monolayer MSCs conditions, and encapsulated MSCs conditions for both immediately after OGD and those collected after the recovery period.

### 3.7 PGE<sub>2</sub>

Supernatants collected after the recovery period was tested for total PGE<sub>2</sub> levels. Figure 13 shows the normalized levels of PGE<sub>2</sub> for each duration of OGD, control, monolayer MSCs and encapsulated MSCs treatment.

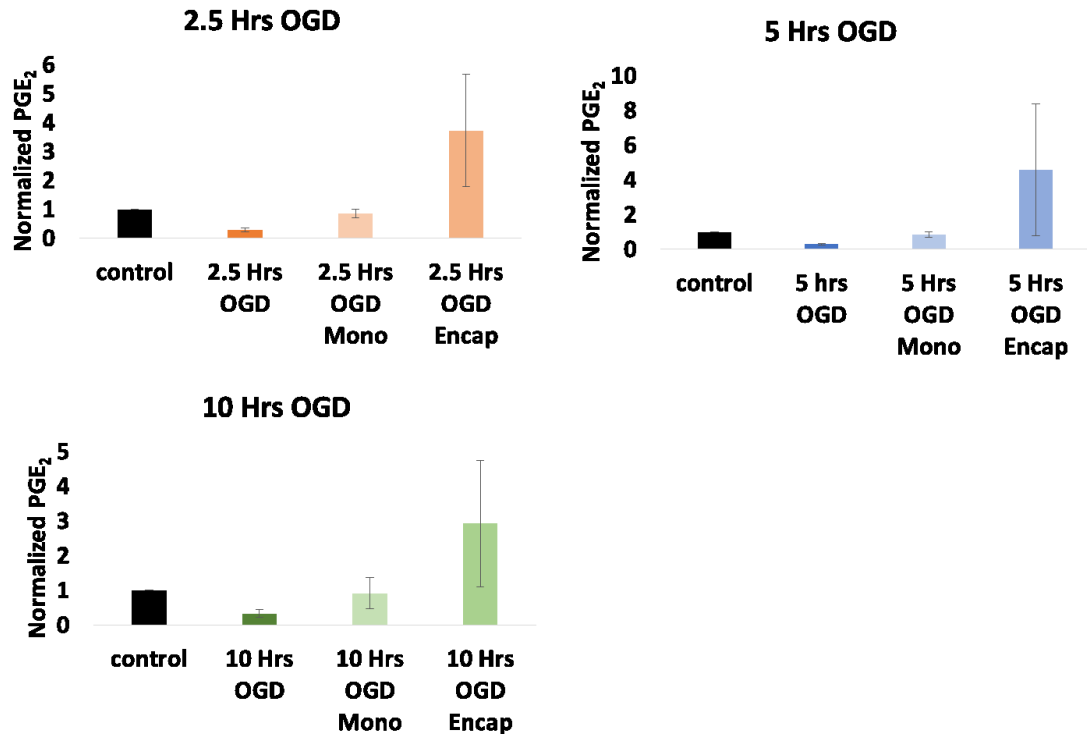


**Figure 13.** Total PGE<sub>2</sub> levels for 2.5, 5, and 10 hours of OGD for control, monolayer MSCs, and encapsulated MSCs. PGE<sub>2</sub> levels are normalized to control.

In OGD only, total PGE<sub>2</sub> or PGE<sub>2</sub> produced by astrocytes was reduced compared to control. Monolayer MSCs treatment restored total PGE<sub>2</sub> levels to control. Encapsulated MSCs increased total PGE<sub>2</sub> above control levels. Since total PGE<sub>2</sub> was measured, the amount of PGE<sub>2</sub> is a combination of PGE<sub>2</sub> produced by both the astrocytes and the MSCs. Therefore, monolayer MSCs and encapsulated MSCs total PGE<sub>2</sub> levels could be the addition of PGE<sub>2</sub> that MSCs make.

To further determine if PGE<sub>2</sub> produced by MSCs are responsible for the changes in astrocytes, exogenous PGE<sub>2</sub> was added during the recovery period instead of MSCs. Figure 14 shows the GFAP stained astrocytes with and without exogenous PGE<sub>2</sub>. Visually there does not seem to be a difference in GFAP intensity or morphology between OGD only and exogenous PGE<sub>2</sub>.

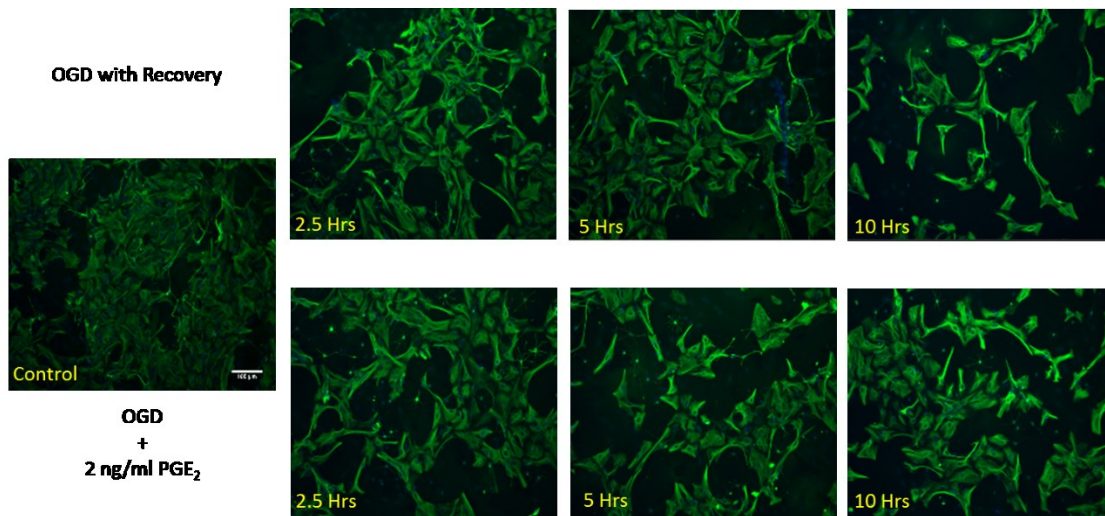


**Figure 14.** GFAP immunostaining (green) and DAPI (blue) for astrocytes treated with and without exogenous PGE<sub>2</sub>. Representative images for each condition are shown. Images for 2ng/ml of PGE<sub>2</sub> were chosen since this was near the total PGE<sub>2</sub> level seen in the supernatant.

In order to see if there is a dose response to PGE<sub>2</sub>, exogenous PGE<sub>2</sub> of 0, 1, 2, 8, and 16 ng/ml was added during the recovery period. For each duration, astrocytes were stained for GFAP and analyzed. Figure 15 shows the GFAP intensity analysis. For each duration of OGD, there is no significant difference in GFAP intensity with the different dosage compared to OGD only.

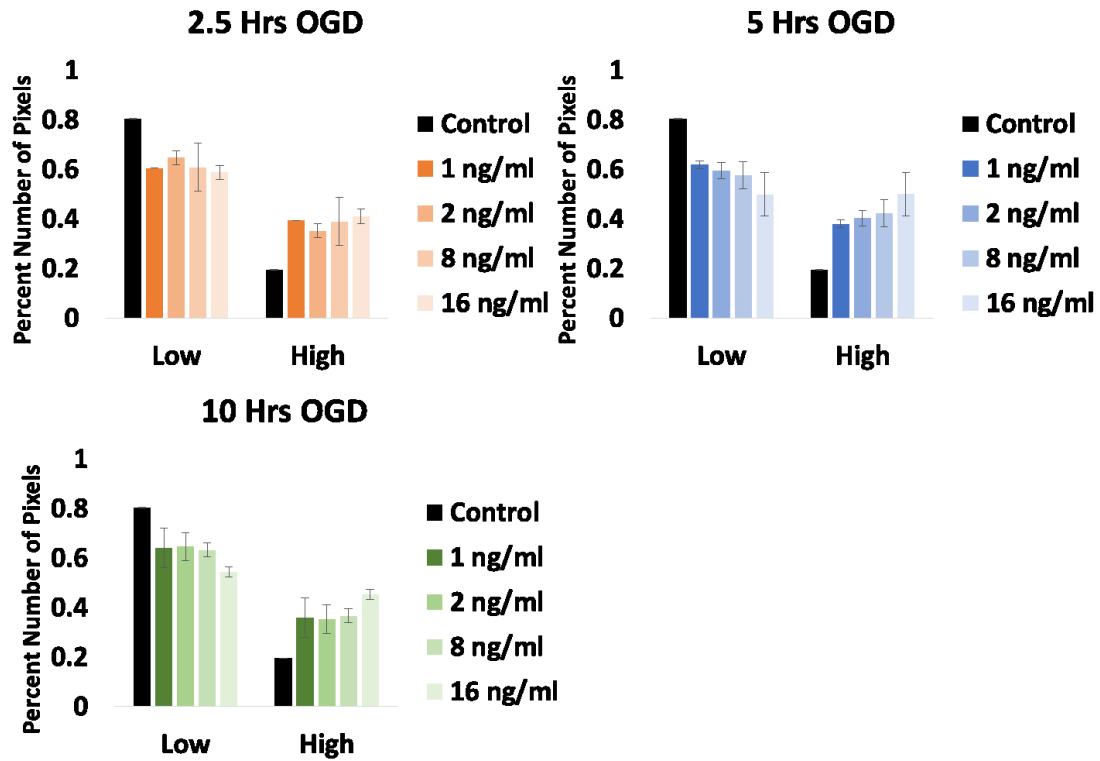


**Figure 15.** GFAP intensity analysis of astrocytes after being exposed to exogenous PGE<sub>2</sub> during the recovery period. Concentrations of 0, 1, 2, 8, and 16 ng/ml of PGE<sub>2</sub> were used.

Exogenous PGE<sub>2</sub> did not change GFAP intensity even after going above the total PGE<sub>2</sub> levels observed with encapsulated MSCs. This means that PGE<sub>2</sub> is not responsible for the changes seen with MSCs treatment.



## CHAPTER 4: DISCUSSION

### 4.1 OGD

As astrocytes become more and more of the focus in brain injuries, their role continues to evolve and new information is gained. Astrocytes role during stroke is not one that is well understood, however, there are previous experiments exposing astrocytes to a stroke environment *in vitro* through an OGD system. However, the method of creating an OGD environment is not consistent between research groups, creating a wealth of knowledge which doesn't always agree with each other<sup>15, 16</sup>. Therefore, it is currently necessary for each lab group to create their own baseline OGD system. In this system a 1% O<sub>2</sub> OGD system was used. With this system we found several interesting characteristics of astrocytes during OGD which generally agree with the literature.

The activation of astrocytes is an expected result of putting astrocytes into an OGD environment which is supposed to mimic an injury. With the activation of astrocytes there is an increase in GFAP expression. However, the unexpected result is that there is no time dependent increase in GFAP as seen in Figure 3. There are several possible reasons for this. One reason possible reason is the control over the actual O<sub>2</sub> levels. All the time points were done in the same incubator, however, even briefly opening the incubator to take samples in or out dramatically increased the O<sub>2</sub> percentage briefly. This intermediate increase in O<sub>2</sub> could be a possible explanation for the lack of a time dependent result. If greater control of the O<sub>2</sub> level were possible with our current system, it is hypothesized that a time dependent increase in GFAP would be observed. Another possible reason is that the GFAP expression has reached a steady state after 2.5 hours and that if an earlier time point would be used then a time dependent GFAP expression would be seen.

In our system, the astrocytes also went under a change in morphology. Astrocytes forming glial scars during brain injury is known. In *in vitro* systems, this change in morphology is not well documented. There are few papers trying to characterize the morphology of astrocytes during injury. At most, papers will make note of the change in morphology, but will not try to characterize it<sup>17</sup>. In this paper, we used a perimeter over area ratio to characterize the shape of the astrocytes following a previous paper that used the same method<sup>18</sup>. Interestingly, with the morphology, there was a time dependent change in the perimeter to area ratio with astrocytes although not significantly different between OGD durations as seen in Figure 6. There is a need to establish a common method for analyzing astrocyte morphology, which is not as simple as other cell types do to the branching of astrocytes.

#### **4.2 MONOLAYER MSCs VS ENCAPSULATED MSCs**

The result of these experiments is the modulation of GFAP and morphology by the MSCs. The expected result was that the MSCs would modulate GFAP and morphology changes because in previous experiments of using MSCs were able too<sup>19</sup>. Monolayer and encapsulated MSCs treatment worked on a similar level for both the GFAP reduction and the reduction in the perimeter to area ratio. The interesting result here is that the encapsulated only worked as well as the monolayer treatment. In previous experiments the encapsulated MSCs worked significantly better than the monolayer<sup>19</sup>. This made us wonder what is different in this system compared to the previous systems.

One the main differences was that the previous systems all had TNF- $\alpha$  in the system. This is an inflammatory molecule to which the MSCs can react to. The astrocytes in the OGD system were not producing any TNF- $\alpha$ . One possibility is that no molecule is attaching to the astrocyte cell surface to tell the astrocyte to produce TNF- $\alpha$ . This OGD model is a simplified system without neurons and other neuronal cells. In a more complex system with neurons, the neurons would

release various factors such as glutamate and other neurotransmitters which could cause for the astrocytes to produce TNF- $\alpha$ . This in turn could cause for the MSCs to respond more strongly and therefore respond as previously seen with other systems.

### 4.3 PGE<sub>2</sub> RESPONSE

Even though the monolayer and encapsulated MSCs created a similar result, PGE<sub>2</sub> was investigated as the molecule of interest since PGE<sub>2</sub> was the main molecule responsible in previous systems. However, in the OGD system there was only a small fold increase in PGE<sub>2</sub> levels compared to monolayer and control as seen in Figure 13. In a system where the astrocytes were treated with LPS, monolayer MSCs produced about 7 ng/ml and encapsulated MSCs produced about 8 ng/ml of PGE<sub>2</sub><sup>19</sup>. To further confirm that PGE<sub>2</sub> was not responsible for the changes that were observed, exogenous PGE<sub>2</sub> was added during the recovery phase. With the exogenous PGE<sub>2</sub> there was no change in the GFAP expression confirming that PGE<sub>2</sub> is not responsible for the changes.

The mechanism of action of how the MSCs are affecting the astrocytes is still unknown. Previous experiments have shown that the p38/ MAP JNK are downregulated when monolayer MSCs are used as a treatment<sup>17</sup>. This pathway is activated by growth factors or inflammatory molecules. Therefore, the MSCs must be producing something to either block this pathway or reduce the production of a growth factor or molecule that the astrocytes are producing due to the OGD injury.

### 4.4 *IN VIVO* STUDIES

There are two types of strokes modeled in *in vivo*, global and focal. Global involves blocking carotid arteries or other major arteries leading to the brain while focal blocks the arteries in the brain and the blockage is maintained for about 15 minutes<sup>20</sup>. However, the focus has shifted towards focal stroke model because it mimics strokes more closely. There are several different methods for inducing *in vivo* focal stroke. One common method is to clamp off the major arteries

such as the middle cerebral arterial occlusion (MCAo)<sup>21</sup>. This can be done by suturing the artery or by tying it off with nylon string and lasting for about 2 hours. A more recent method is to use a photosensitive chemical to create the stroke. When a light source at a specific wavelength is aimed towards a region in the brain, the photosensitive chemical reacts creating a thrombosis<sup>22</sup>. Evaluating the extent of the stroke and the secondary effects are critical for determining if a treatment works. Histology is used to determine the size of the infarction as well as looking at the composition of the tissue, such as, myelination, number of neurons, or neuronal stem cells as a few examples. Cell type markers are also used to determine the types of cell present around the injury. SDF-1/CXCR-4 have been used to determine the extent of migration of native neural stem cells.<sup>6</sup> Neuronal nuclei (NeuN), microtubule associated protein 2 (MAP2) and synapsin are other markers used to characterize the injury site<sup>23</sup>.

MRI allows for physiological information to be directly linked to the anatomical characteristics in the area of the injury. This can be done by tracking the energy demands of the tissue. After a stroke, there will be a decrease in activity as the tissue dies and then a subsequent increase as there is an infiltration of immune cells and neural stem cells<sup>23</sup>. Additional information about the tissue can be obtained by combining MRI with other tools such as the use of manganese to see synaptic connectivity<sup>23</sup>.

To determine effectiveness of treatment and the extent of the injury *in vivo*, behavioral tests were done. These tests look to quantify the neurological condition of the animals along with the motor function. Neurological tests are subjective at times and performed by looking at typical animal behavior such as eating habits and other interactions with the environment. Examples of motor function tests are rotarod test, beam walking, and grip strength<sup>21, 22, 24</sup>. Furthermore, the size of infarction is examined via histology. The rotarod test is where the rodent is placed on a

rotating rod where the speed of rotation is slowly increased to 20 RPM and last 3 minutes. The speed and duration were selected so that control animals would not fall off<sup>22</sup>.

In one study, while investigating the inflammatory response, the p38 and MAPK was found to be upregulated after injury<sup>22</sup>. Another study found that there was an increase in neurite outgrowth and myelin after stroke with MSCs treatment. This was attributed to an increase in tissue plasminogen activator (tPA) in astrocytes<sup>25</sup>. MSCs also has the potential to differentiate towards neuro-like cells. Additionally paracrine factors secreted by MSCs such as BDNF have proven to help neurite outgrowth. Ischemic MSCs was compared against normal MSCs in order to determine if MSCs could be obtained from a stroke patient. It was found that ischemic MSCs performed as well as normal MSCs when looking at neuronal connection and increasing neuronal survivability<sup>21</sup>.

Similar effects have been seen with MSCs with other central nervous system injuries. In an experiment where the lumbar ventral roots of a rat were crushed, a MSCs treatment was applied and increased the survivability of neurons and their connections compared to no treatment. Furthermore, there was a decrease in GFAP expression in astrocytes at the injury site<sup>26</sup>. In a spinal cord injury model, encapsulated MSCs were found to have modulate inflammatory response by changing the phenotype of macrophages from a M1 to a M2 state which lead promoted tissue regeneration<sup>8</sup>. These results suggest that MSCs can be an effective therapeutic in a wide range of central nervous system injuries.

#### **4.5 FUTURE STUDIES**

This thesis shows that MSCs has an effect on GFAP and morphology of astrocytes that have been exposed to OGD. However, I was unable to determine the mechanism of action of how the MSCs was doing this. As previously stated, it is possible that a growth factor or cytokine that

the astrocytes produce are being reduced. However, what molecule or molecules that the MSCs are producing this is still unknown. One possible way to reduce the number of possibilities is to look at an array of common molecules produce by the MSCs and see if there are any significant changes. This could also be applied to astrocytes in order to determine what growth factors or cytokines are being reduced if any.

Additionally, this thesis used a very basic model. In order to fully gauge the potential of the MSCs to help during stroke, a more complex model needs to be used such as a tri-culture with neurons. This type of system might make the astrocytes produce TNF- $\alpha$  allowing for a greater response from the MSCs as previously seen. Another step above this would be going to an organotypic slice culture model. This type of model retains many of the neuronal cell types and brain structure without doing an *in vivo* study. Ultimately, if there are still benefits seen in the more complex models, *in vivo* studies would be performed to confirm efficacy of the encapsulated MSCs.

## REFERENCES

1. "Stroke Warning Signs and Symptoms." Stroke Warning Signs and Symptoms. N.p., n.d. Web. 16 Oct. 2016.
2. Silver, Jerry, Miller, Jared. "Regeneration Beyond the Glial Scar", *Nature reviews neuroscience*, 5; 145-156, 2004 Feb.
3. Bélanger, Mireille, and Pierre J. Magistretti. "The Role of Astroglia in Neuroprotection." *Dialogues in Clinical Neuroscience* 11.3 (2009): 281–295. Print.
4. Sofroniew, Michael V. "Reactive Astrocytes in Neural Repair and Protection." *Neuroscientist*, 2005 11(5), 400-407.
5. Sofroniew MV, Vinters HV. Astrocytes: biology and pathology. *Acta Neuropathologica*. 2010;119(1):7-35.
6. Mayo Clinic Staff. "Treatment." *Stroke*, 10 Aug. 2016
7. Zhang, Run et al. "Anti-Inflammatory and Immunomodulatory Mechanisms of Mesenchymal Stem Cell Transplantation in Experimental Traumatic Brain Injury." *Journal of Neuroinflammation* 10 (2013): 106. PMC. Web. 16 Oct. 2016.
8. Barminko, J., Kim, J. H., Otsuka, S., Gray, A., Schloss, R., Grumet, M. and Yarmush, M. L. (2011), Encapsulated mesenchymal stromal cells for in vivo transplantation. *Biotechnol. Bioeng.* 108: 2747–2758. doi: 10.1002/bit.23233
9. Middeldorp, J, Hol, E.M., "GFAP in Health and Disease", *Progress in Neurobiology*, 93(3), 2011 Mar, 421-443.
10. Yagi, Hiroshi et al. "Mesenchymal Stem Cells: Mechanisms of Immunomodulation and Homing." *Cell transplantation* 19.6 (2010): 667–679. PMC. Web. 10 Nov. 2016.
11. Alginate micro-encapsulation of mesenchymal stromal cells enhances modulation of the neuro-inflammatory response
12. Gu, Y., et al. (2016). "Endogenous IL-6 of mesenchymal stem cell improves behavioral outcome of hypoxic-ischemic brain damage neonatal rats by suppressing apoptosis in astrocyte." *Scientific Reports* 6: 18587
13. Petroski RE, et al. "Basic fibroblast growth factor regulates the ability of astrocytes to support hypothalamic neuronal survival in vitro." *Developmental Biology* 1991; 147:1–13.
14. Kai Murk, Elena M. Blanco Suarez, Louisa M. R. Cockbill, Paul Banks, Jonathan G. Hanley *J Cell Sci* 2013 126: 3873-3883
15. Wei, Shuyong, et al. "Pathways Involved in Oxygen Glucose deprivation Damage of Astrocytes." *Journal of Molecular Neuroscience* 2016 Sep 6.
16. Wang, Liang, et al. "Neuroprotective Effect of Neuroserpin in Oxygen-Glucose Deprivation- and Reoxygenation-Treated Rat Astrocytes In Vitro." *PLoS ONE* 10(4): e0123932. doi:10.1371/journal.pone.0123932
17. Huang, W., et al. "Paracrine Factors Secreted by MSCs Promote Astrocyte Survival Associated with GFAP Downregulation after Ischemic Stroke via p38 MAPK and JNK." *J. Cell. Physiol.*, 2015, 230: 2461–2475.
18. Murk, Kai, et al. "The Antagonistic modulation of Arp2/3 Activity by N-Wasp, Wave2 and PICK1 Defines Dynamic Changes in Astrocyte Morphology." *Journal of Cell Science* 2013 126: 3873-3883
19. Stucky, EC, et al. "Alginate Micro-encapsulation of Mesenchymal Stromal cells Enhances Modulation of Neuro-inflammatory Response." *Cytotherapy*. 2015 Oct; 17(10).
20. Tajiri, Naoki et al. "In Vivo Animal Stroke Models: A Rationale for Rodent and Non-Human Primate Models." *Translational stroke research* 4.3 (2013): 308–321.

21. Tsai, May-Jywan et al. "Recovery of Neurological Function of Ischemic Stroke by Application of Conditioned Medium of Bone Marrow Mesenchymal Stem Cells Derived from Normal and Cerebral Ischemia Rats." *Journal of Biomedical Science* 21.1 (2014): 5.
22. Choi, Y.-K., Urnukhsaikhan, E., Yoon, H.-H., Seo, Y.-K. and Park, J.-K. (2016), Effect of human mesenchymal stem cell transplantation on cerebral ischemic volume-controlled photothrombotic mouse model. *Biotechnology Journal*, 11: 1397–1404.
23. Gervois, P., Wolfs, E., Ratajczak, J., Dillen, Y., Vangansewinkel, T., Hilkens, P., Bronckaers, A., Lambrichts, I. and Struys, T. (2016), Stem Cell-Based Therapies for Ischemic Stroke: Preclinical Results and the Potential of Imaging-Assisted Evaluation of Donor Cell Fate and Mechanisms of Brain Regeneration. *Med. Res. Rev.*, 36: 1080–1126.
24. Quittet, Marie-Sophie, et al. "Effects of mesenchymal stem cell therapy, in association with pharmacologically active microcarriers releasing VEGF, in an ischaemic stroke model in the rat", *Acta Biomaterialia*, March 2015, 15: 77-88.
25. Xin, Hongqi et al. "Increasing tPA Activity in Astrocytes Induced by Multipotent Mesenchymal Stromal Cells Facilitate Neurite Outgrowth after Stroke in the Mouse." Ed. Henning Ulrich. *PLoS ONE* 5.2 (2010): e9027.
26. Spejo, A. B., et al. "Neuroprotective effects of mesenchymal stem cells on spinal motoneurons following ventral root axotomy: Synapse stability and axonal regeneration." *Neuroscience*, 2013-10-10, 250, 715-732.



## APPENDIX

### MATLAB CODE FOR IMAGE ANALYSIS

```

1%% to get all images in a folder
imgpath=input('please input the folder name: ','s');
group=input('please enter the number of groups ');
pic=input('please enter the number of pics per group ');
dcell = dir(imgpath);
cd(imgpath)
for d = 3 :1: length(dcell)
    seq{d-2} = imread([ dcell(d).name]);
end
cd ..
k=1;
number=length(seq);
countst=0;
%% Determine bins
spacing=[330,482];
numbins=length(spacing);
avecounts=zeros(group*pic,length(spacing));
averagecounts=zeros(group,length(spacing));
m=1;
%% loop through all images
for k=1:1:number
    %threshold the image
    bw=im2bw(seq{1,k},330/65536);
    test1=uint16(bw);
    y=test1.*seq{1,k};
    i=1;
    j=1;
    intensity=0;
    counter=0;
    %get intensity value from images
    for i=1:1:1024
        for j=1:1:1344
            if y(i,j)==0
            else
                intensity= double(y(i,j)) + double(intensity);
                counter=counter+1;
            end
        end
    end
    yold=y;
    y=double(y(:));
    i=1;
    %set zeros to NAN
    for i=1:1:1376256

```

```

        if y(i,1)==0
            y(i,1)=NaN;
        end
    end
    %%
    %%find histogram of each threshold image, then add them up
    if k<=pic*m
        [counts bins]=hist(y(:),spacing);
        %normalize data
        totalpix(m)=sum(counts);
        avecounts(k,:)=counts./totalpix(m);
        %% gets data for statistical analysis
        stat(k-(pic*(m-1)),(1+numbins*(m-1)):(numbins*m))=counts./totalpix(m);
        %adds up the number of points per bin
        countst=counts+countst;
        if k==pic*m
            averagecounts(m,:)=mean(avecounts(k-(pic-1):k,:));
            standardev(m,:)=std(avecounts(k-(pic-1):k,:));
            m=m+1;
        end
    end
    intensityav=intensity/counter;
    final{1,j}= yold;
    intensityvalues(k,1)=intensityav;
    intensityvalues(k,2)=counter;
    if k==pic*(m-1)
        intsav(m-1,1)=mean(intensityvalues(k-(pic-1):k,1));
        intsav(m-1,2)=std(intensityvalues(k-(pic-1):k,1));
    end
end
%% getting statistics
[p,~,stats]=anova1(stat,[],'off');
c=multcompare(stats);

```